

Our analysis offers insights into the selective forces that shape coloration. Unlike open-nesting birds, in which the incubating females need to be inconspicuous to avoid predation, females of hollow-nesting species usually have similar colors to males. The sharing of parental duties and similar exposure to predation (during incubation and foraging) suggest that natural selection affects color similarly in both sexes in most species (22, 23). In contrast, the colors of male and female *E. roratus* appear to be under independent selection. Whereas females are more conspicuous than males against leaves, they also have the nest hollow nearby as a refuge against predators. However, foraging males cannot retreat to a nest hollow whenever a predator approaches, and consequently their colors need to be less conspicuous against the leafy background. Ready access to a refuge from predators may also explain why females are not less conspicuous from above (Fig. 1A) or why they do not have colors that are significantly less conspicuous to their aerial predators (Fig. 1E).

The continuous occupation of the nest hollow by female *E. roratus* is atypical for parrots (11) but strikingly similar to that seen in hornbills (Bucerotiformes) (24). Females in most hornbill species are sealed into the nest hollow during the incubation and nestling phases and are fed by their mates and other group members. However, strong sexual dichromatism is rare in this group (24). Unlike *E. roratus*, most hornbill species (25 out of 33 known) are territorial, and the males and females of all 41 species on which sufficient data have been gathered have been observed to locate, prepare, and defend the nest site together. Further, female hornbills often leave the nest and help provision young before the young have fledged (24) and overall do not remain at the hollow for as long (66 to 142 days as compared with 279 days in *E. roratus*) (24). Similar sex roles both before and during breeding, and less total time spent at the nest by females, may reduce any independent selection on each sex in hornbills.

In *E. roratus*, a rare combination of intrasexual competition for a scarce resource in females, the separation of parental duties, and visually mediated predation appears to have shifted the balance of natural and sexual selection from the expected monomorphism in hollow nesters toward reversed dichromatism. These parrots provide an example of how conspicuous colors, like complex song (25), can result from strong intrasexual competition. The dichromatism of these parrots is also highly unusual among birds (8) because the sexes have acquired different color patterns for different purposes, and each is more conspicuous under specific conditions. Females compete for nest hollows and males compete for fe-

males at nest hollows, and thus both sexes are conspicuous against the tree trunks. However, males differ from females by spending a much larger proportion of their time foraging among the rainforest canopy. This favors reduced visibility to predators against leaves and, as a result, the balance between sexual selection and predation (26, 27) differs in the two sexes and represents a reversal of the usual pattern. Although theory successfully predicts the direction of sexual selection (9, 26–29), and mutual mate choice can account for similarly adorned sexes (30), *E. roratus* shows that bright coloration can evolve independently and simultaneously in both sexes. *Erectus* parrots emphasize the crucial interaction between natural selection and the lifestyle of males and females in modifying colors, even if they primarily result from sexual selection.

#### References and Notes

- M. Andersson, *Sexual Selection* (Princeton Univ. Press, Princeton, NJ, 1994).
- C. Kvarnemo, I. Ahnesjö, *Trends Ecol. Evol.* **11**, 404 (1996).
- V. C. Almada, E. J. Gonçalves, R. F. Oliveira, A. J. Santos, *Anim. Behav.* **49**, 1125 (1995).
- M. Eens, R. Pinxten, *Behav. Processes* **51**, 135 (2000).
- T. Székely, R. P. Freckleton, J. D. Reynolds, *Proc. Natl. Acad. Sci. U.S.A.* **101**, 12224 (2004).
- J. M. Forshaw, W. D. Cooper, *Parrots of the World* (Lansdowne Press, Willoughby, Australia, 1989), pp. 616.
- A. Grafen, *The Guardian*, 9 March 2000, p. 27.
- T. Amundsen, H. Parn, in *Avian Coloration*, G. E. Hill, K. J. McGraw, Eds. (Harvard Univ. Press, Boston, in press).
- S. T. Emlen, L. W. Oring, *Science* **197**, 215 (1977).
- R. Heinsohn, S. Legge, *J. Zool.* **259**, 197 (2003).
- T. Juniper, M. Parr, *Parrots: A Guide to Parrots of the World* (Pica Press, Sussex, UK, 1998).
- S. Legge, R. G. Heinsohn, S. Garnett, *Wildl. Res.* **31**, 149 (2004).
- R. Heinsohn, S. Murphy, S. Legge, *Aust. J. Zool.* **51**, 81 (2003).
- We found eggs crushed but not eaten in 33 out of

421 clutches. In seven cases, the crushed eggs were found immediately after we saw an intruding female leave the nest hole. Ovicide was inferred in the remaining 26 cases. A 21-day-old nestling was found dead with wounds apparently inflicted by a parrot beak after an intruding male left the nest. We inferred infanticide in 15 further nests where nestlings aged from 1 to 15 days were found dead with similar wounds. One adult female was found dead in her hollow with extensive wounds on her head after an extended fight with an intruding female. Thirteen other uneaten corpses of adult females were found in the vicinity of nest trees in 210 female-years. Ten of these had wounds consistent with fighting.

- J. A. Endler, *Biol. J. Linn. Soc.* **41**, 315 (1990).
- A. T. D. Bennett, I. C. Cuthill, *Vision Res.* **34**, 1471 (1994).
- Materials and methods are available as supporting material on Science Online.
- J. A. Endler, P. W. Mielke, *Biol. J. Linn. Soc.*, in press.
- J. A. Endler, *Ecol. Monogr.* **63**, 1 (1993).
- J. A. Endler, M. Thery, *Am. Nat.* **148**, 421 (1996).
- J. A. Endler, *Vision Res.* **31**, 587 (1991).
- A. R. Wallace, *Darwinism* (Macmillan, London, ed. 2, 1889).
- R. R. Baker, G. A. Parker, *Philos. Trans. R. Soc. London Ser. B* **287**, 63 (1979).
- A. Kemp, *The Hornbills* (Oxford Univ. Press, Oxford, 1995).
- N. E. Langmore, *Trends Ecol. Evol.* **13**, 136 (1998).
- J. A. Endler, *Evol. Biol.* **11**, 319 (1978).
- J. A. Endler, *Evol. Int. J. Org. Evol.* **34**, 76 (1980).
- T. H. Clutton-Brock, A. C. J. Vincent, *Nature* **351**, 58 (1991).
- H. Kokko, P. Monaghan, *Ecol. Lett.* **4**, 159 (2001).
- I. L. Jones, F. M. Hunter, *Nature* **362**, 238 (1993).
- We thank C. Blackman, A. Cockburn, N. Doerr, M. Hall, P. and E. Huybers, M. Jennions, N. Langmore, S. Murphy, A. Nathan, S. Rothstein, D. Storch, and D. Wilson, and the Australian Research Council and National Geographic Society.

#### Supporting Online Material

www.sciencemag.org/cgi/content/full/309/5734/617/DC1

Materials and Methods

Fig. S1

Table S1

References

25 March 2005; accepted 17 May 2005  
10.1126/science.1112774

## Independent Codes for Spatial and Episodic Memory in Hippocampal Neuronal Ensembles

Stefan Leutgeb,<sup>1</sup> Jill K. Leutgeb,<sup>1</sup> Carol A. Barnes,<sup>1,2</sup>  
Edvard I. Moser,<sup>1</sup> Bruce L. McNaughton,<sup>1,2\*</sup> May-Britt Moser<sup>1</sup>

Hippocampal neurons were recorded under conditions in which the recording chamber was varied but its location remained unchanged versus conditions in which an identical chamber was encountered in different places. Two forms of neuronal pattern separation occurred. In the variable cue-constant place condition, the firing rates of active cells varied, often over more than an order of magnitude, whereas the location of firing remained constant. In the variable place-constant cue condition, both location and rates changed, so that population vectors for a given location in the chamber were statistically independent. These independent encoding schemes may enable simultaneous representation of spatial and episodic memory information.

Hippocampal neuronal ensemble activity appears to play an important role in the establishment of both spatial and nonspatial episodic memories, but there has long been

controversy as to which of these parameters best characterizes the role of the hippocampal formation in mnemonic processes (1, 2). Although hippocampal neurons fire in a sparse

(3), spatially selective (4, 5) manner, this activity can be weakly or strongly affected by other variables such as directional orientation (6, 7), specific sensory inputs (8–11), behavioral context (12–17), and working memory (11, 14–17). “Place fields” of a given neuron may change in magnitude, shift in position, or appear or disappear under different circumstances. All of these effects have been subsumed under the general terms “remapping” (18–20) or “orthogonalization” (3, 21, 22), but it has not been determined whether these effects can occur independently across simultaneously recorded neurons. Here, we show that the hippocampal population vector can undergo two essentially independent forms of remapping: rate remapping, in which the locations of place fields remain unchanged but the firing rates of the cells change, and global remapping, in which the distributions of location and rate both take on statistically independent values. In vector terms, rate remapping implies that the population vectors span the same subspace and hence preserve information about location, whereas in global remapping the population vectors span statistically independent subspaces. In principle, rate remapping permits the generation of representations of unique episodes of experience while maintaining the integrity of the code for spatial location, whereas global remapping permits the distinction between similar experiences that occur in different spatial contexts.

Ensemble activity was recorded from 330 cells in CA3 and 487 cells in CA1 of the dorsal hippocampus in 10 freely moving rats by using arrays of 12 tetrodes, about half of which were located in CA3 and half in CA1 (23). Two experimental conditions were studied. In the variable cue-constant place condition (Fig. 1), the recordings were conducted in a single room, but the actual recording chamber was varied, either by changing the shape (circular versus square) or by changing the wall color (black versus white). In the variable place-constant cue condition (Fig. 2), geometrically identical (square) chambers of the same color (black) were used in two distinct rooms. All rats were familiarized with the experimental protocols and conditions before recording (24).

For each cell whose mean firing rate in at least one environmental condition was above an estimate of background noise (25), we compared the location and rate of firing in the different experimental configurations. Spatial similarity was expressed by computing

the correlations between pairs of rate maps and comparing their centers of mass. These measures are independent of the relative

magnitude of firing. Rate similarity was expressed by dividing the relative change in mean rate by the sum of the mean rates.

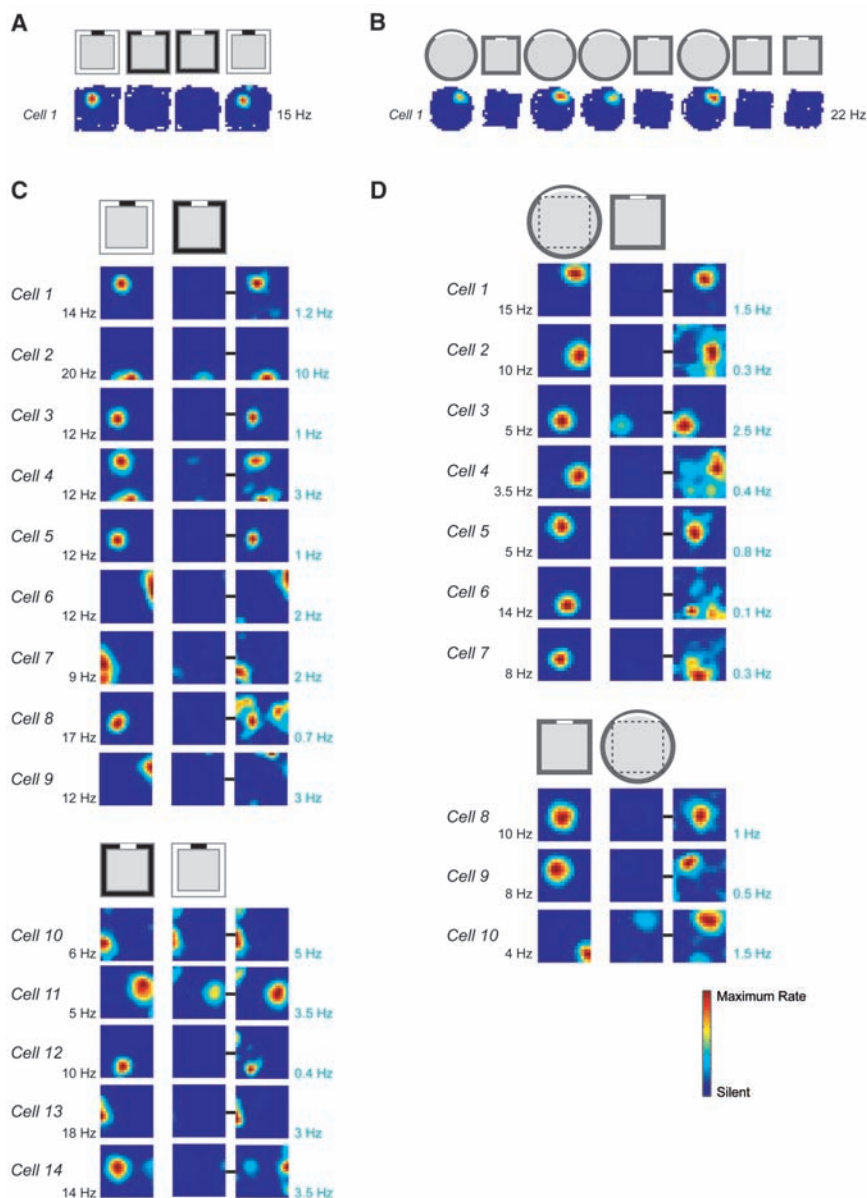


**Fig. 1.** Constant place-variable cue condition. Color-coded rate maps for cells recorded when the cue configuration was changed by switching either between two colors (A and C) or between two shapes (B and D) at a constant location. (A and B) Recording sequence with the rate maps of the first cell in (C) and (D) as an example. Rate is coded on a color scale from blue (silent) to red (maximum rate). Pixels not sampled are white. The symbols above the maps indicate color and shape of the box and the cue card (cue card in contrasting color). (C and D) Rate maps for two complete sets of simultaneously recorded CA3 neurons [(C) rat 10708, day 3; (D) rat 10683, day 16]. Repeated trials with the same cues are now averaged. In (D), only the area common to both shapes is shown (indicated by the dotted square in the circle). Only the area common to both shapes is depicted. Each row shows data from one active neuron. Silent cells [six in (C) and six in (D)] are not shown. The left columns show data for the condition that gave maximal firing. For each cell, the rate scale corresponds to the peak firing rate in that condition (indicated to the left of the rate map). In the middle columns, the data from the opposite condition are plotted at the same firing-rate scale. The right columns contain the same data as the middle but are scaled to their own maximum values (indicated to the right of the rate maps). Symbols above columns indicate which color or shape gave the higher and lower rate (left and middle, respectively) for the cells underneath. Note that different experiences in the same place resulted in place fields similar in location and shape, but with strikingly different firing intensities, sufficient, in many cases, to make it appear that the field was absent when plotted at the same scale. See fig. S2 for rate maps of individual trials and fig. S4, A and B, for rate maps of simultaneously recorded CA1 cells.

<sup>1</sup>Centre for the Biology of Memory, Medical-Technical Research Centre, Norwegian University of Science and Technology, 7489 Trondheim, Norway. <sup>2</sup>Arizona Research Laboratories Division of Neural Systems, Memory, and Aging, University of Arizona, Tucson, AZ 85724, USA.

\*To whom correspondence should be addressed.

Lastly, representational similarity in the population as a whole was estimated by stacking all rate maps (including those of the silent cells) into a three-dimensional matrix with the two spatial dimensions on the *x* and *y* axes and cell identity on the *z* axis (fig. S1C). The distribution of mean rates along the *z* axis for a given *x-y* location represents the population

vector for that location. Comparing the entire set of population vectors between two trials provides an estimate of how much the ensemble code changed.

For both CA3 and CA1, the distributions of spatial correlations in the two variable cue-constant place conditions (i.e., black square versus white square and circle versus square)

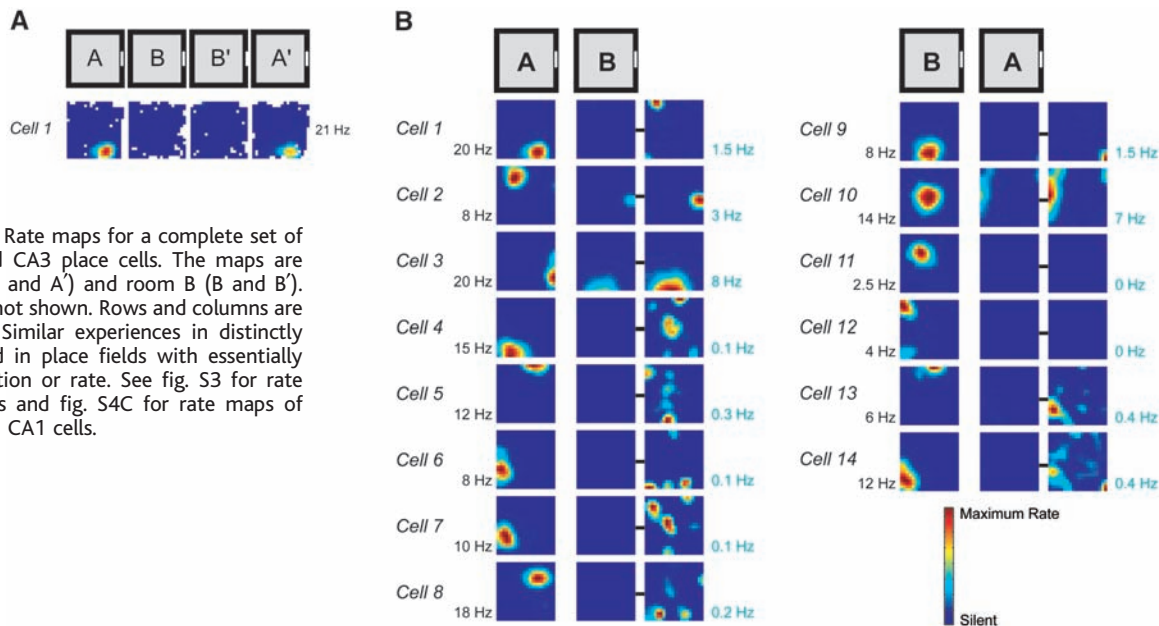
were so similar to the control conditions (first versus second exposure in the same box) that, without closer analysis, one might have concluded that there had been no substantive effect of cue-condition or environmental shape on the hippocampal code (Figs. 1 and 3A and Table 1). In CA3, the median spatial correlations in the black-white and square-circle conditions were 0.82 and 0.83, respectively. In CA1, spatial correlations were similar to those obtained in CA3 (black-white: 0.78, *Z* = 1.54, not significant) or slightly lower (square-circle: 0.65, *Z* = 3.92, *P* < 0.001). In both areas, there were only minor shifts in center of mass of the place fields (Table 1).

In contrast, although the location of firing remained almost constant, the distributions of mean firing rates changed, especially in CA3. In this subfield, a substantial proportion of cells showed pronounced rate differences between conditions, with little or no change in the shape or location of the place field (Figs. 1 and 3A and Table 1). The median rate change between the black and white chambers was 3.9-fold; between square and circle, it was 6.9-fold. The median rate change was significantly higher than that for repeated tests with the same cues (difference/sum ratios; black-white, *Z* = 8.58 and *P* < 0.001; square-circle, *Z* = 7.54 and *P* < 0.001). The change in individual firing rates was also reflected as a pronounced shift toward lower values in the population vector correlations (Fig. 3A and Table 1) (black-white: *Z* = 22.48, *P* < 0.001; square-circle: *Z* = 19.40, *P* < 0.001). In CA1, the changes in relative firing rate were less pronounced (CA3 versus CA1: *Z* was 6.39 and 5.49 for black-white and square-circle, *P* < 0.001) and the population vectors were less different (*Z* was 11.14 and 13.72, respectively, *P* < 0.001) (Fig. 3B and Table 1).

**Table 1.** Spatial firing rate statistics.

| Condition  | CA3              | CA1             |
|--|------------------|-----------------|
| <i>Median place field correlation</i>  |                  |                 |
| Constant cue and place   | 0.94             | 0.88            |
| Color  | 0.93             | 0.87            |
| Shape  | 0.97             | 0.93            |
| Room   | 0.92             | 0.84            |
| Black-white  | 0.82             | 0.78            |
| Circle-square  | 0.83             | 0.65            |
| Room1-room2  | -0.10            | 0.00            |
| <i>Median center of mass change (cm)</i>   |                  |                 |
| Constant cue and place   | 3.3              | 5.6             |
| Color  | 4.3              | 5.9             |
| Shape  | 2.3              | 4.1             |
| Room   | 3.6              | 6.9             |
| Black-white  | 9.8              | 8.6             |
| Circle-square  | 7.4              | 10.2            |
| Room1-room2  | 34.5             | 26.8            |
| <i>Median relative firing rate change (unsigned rate difference divided by rate sum)</i> |                  |                 |
| Constant cue and place   | 0.12 (1.3-fold)  | 0.14 (1.3-fold) |
| Color  | 0.10 (1.2-fold)  | 0.13 (1.3-fold) |
| Shape  | 0.12 (1.3-fold)  | 0.13 (1.3-fold) |
| Room   | 0.14 (1.3-fold)  | 0.16 (1.4-fold) |
| Black-white  | 0.59 (3.9-fold)  | 0.19 (1.5-fold) |
| Circle-square  | 0.74 (6.9-fold)  | 0.30 (1.9-fold) |
| Room1-room2  | 0.97 (61.6-fold) | 0.42 (2.4-fold) |
| <i>Median population vector correlation</i>  |                  |                 |
| Constant cue and place   | 0.91             | 0.83            |
| Color  | 0.91             | 0.85            |
| Shape  | 0.94             | 0.85            |
| Room   | 0.91             | 0.75            |
| Black-white  | 0.58             | 0.73            |
| Circle-square  | 0.24             | 0.57            |
| Room1-room2  | -0.03            | 0.25            |

**Fig. 2.** Variable place-constant cue condition. Color-coded rate maps for tests in identical boxes in two different rooms (rat 10968, day 9). (A) Recording sequence and rate maps with the first cell in (B) as an example. (B) Rate maps for a complete set of simultaneously recorded CA3 place cells. The maps are averages for room A (A and A') and room B (B and B'). Silent cells (*n* = 16) are not shown. Rows and columns are organized as in Fig. 1. Similar experiences in distinctly different places resulted in place fields with essentially zero correlation in location or rate. See fig. S3 for rate maps of individual trials and fig. S4C for rate maps of simultaneously recorded CA1 cells.



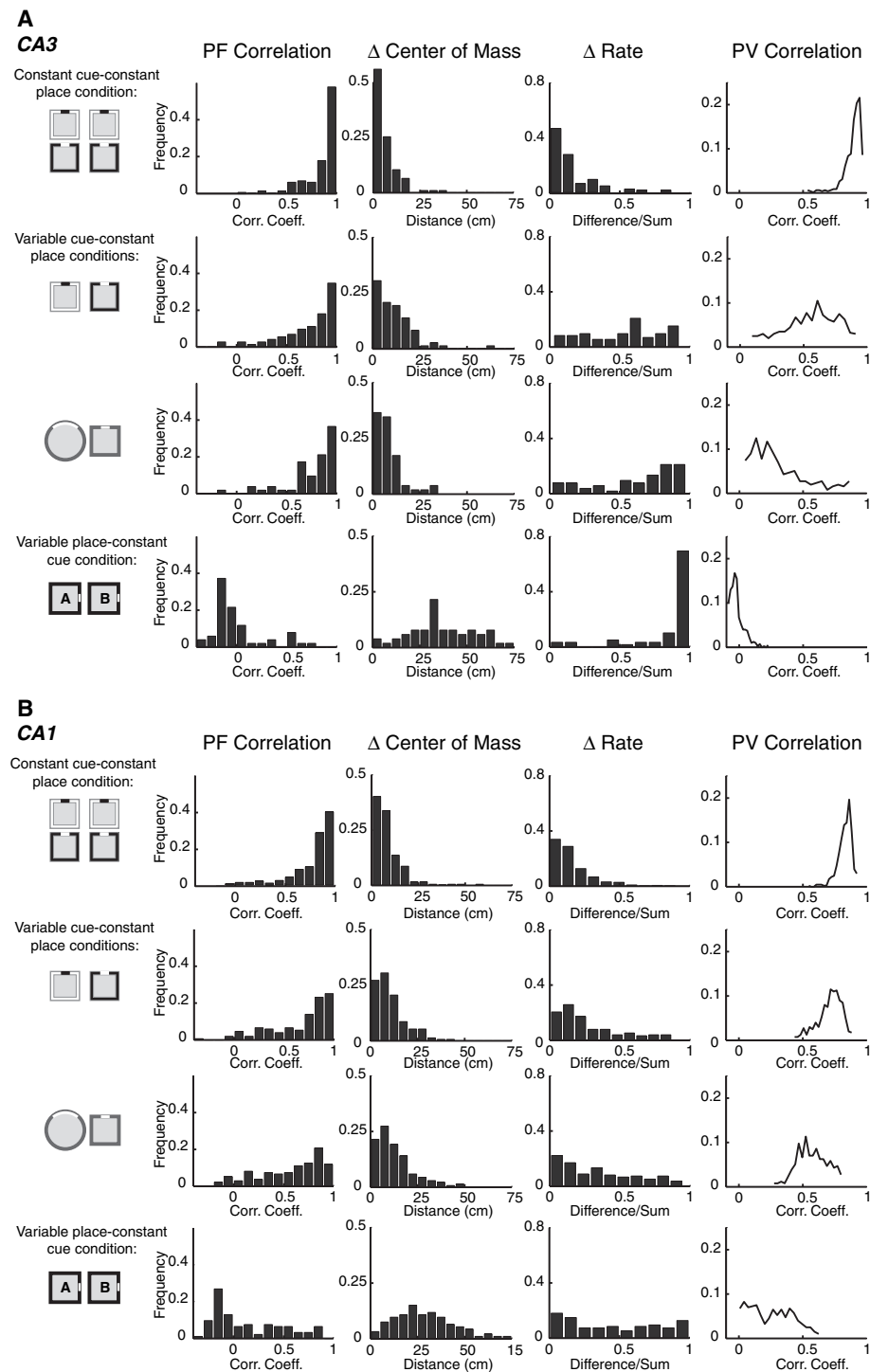


**Fig. 3.** Spatial firing rate statistics for ensembles of hippocampal CA3 (A) and CA1 (B) neurons comparing the following conditions: two visits to the same box in a constant location, visits to black and white boxes in a constant location, visits to circular and square boxes in a constant location, and visits to identical boxes located in two distinctly different places. For each pair of conditions, columns from left to right show frequency distributions for correlations in the spatial firing patterns (PF correlation), shifts of the place-field centers ( $\Delta$  center of mass), changes in the mean firing rates ( $\Delta$  rate), and correlations between spatial population vectors (PV correlation). Rate change is expressed as the unsigned difference between the rates in the two conditions, divided by their sum. On this asymptotic scale, 0.5 corresponds to a threefold difference, whereas 0.8 represents a ninefold difference. Whereas a variable place exerted a marked influence on both rate and firing location, changes in sensory cues in a fixed place resulted only in substantial changes in the firing rates, especially in CA3, with little change in the relative spatial firing distribution, implying that cues and locations are coded independently. See fig. S5 for additional comparisons in the constant cue-constant place configuration.

In the variable place-constant cue condition, the distributions of spatial and population vector correlations were both shifted to values near zero, and the overall firing rate differences were large (Figs. 2 and 3 and Table 1). In CA3, firing locations in the two boxes were totally uncorrelated. Place field correlations were also skewed toward zero in CA1, albeit with a significant tail toward higher values (Fig. 3A) (Kolmogorov-Smirnov test,  $P < 0.05$ ) (Fig. 3B). The change in firing locations was accompanied by pronounced rate changes in the same cells. In CA3, the majority of neurons showed more than 10-fold rate changes, and the population vector correlations for different locations were clustered around zero. In CA1, the extent of rate change varied widely within the population, and population vector correlations ranged between 0 and 0.5. In each animal, the population vectors were more dissimilar in CA3 than CA1.

To summarize, when the same prominent environmental features were encountered in two distinct places, the CA3 population vectors for locations (relative to the reference frame of the constant feature) were uncorrelated. This is consistent with previous studies reporting orthogonalization of hippocampal population activity, especially in CA3, after dislocation of the local reference frame (22, 26–28). When the rats experienced changes in prominent features in the same spatial context, however, the hippocampus encoded these changes primarily by changing the values of the components of the spatial population vectors, without much, if any, change in the distribution of the firing locations (29). The latter finding raises the possibility that much of the previous evidence for single-location remapping is rate-based. Rate remapping may be the cause of direction-specific (6, 30) and trajectory-specific (14–16) firing as well as task-induced changes in population activity (12, 13, 31). However, certain training regimes may provoke global remapping even in a single spatial environment (18–20, 32). Whether the environments are then encoded as distinct spatial reference frames remains to be determined.

The existence of independent population codes for location and cue configurations implies that hippocampal cell ensembles may simultaneously convey information related to where an animal is located and what is currently present in that location. Presynaptic dynamics (33) as well as nonlinear postsynaptic responses may render some neurons sensitive to which inputs are active but not to presynaptic firing rate per se. Cells with such properties might be able to transmit information about the location of the animal irrespective of current sensory input. In contrast, cells that are sensitive to the rate function of afferent neurons might discriminate different events occurring at a given location. The pres-

ervation of both types of information in the hippocampal output may form the basis of its key role in episodic memory (2, 34).

### References and Notes

- J. O'Keefe, L. Nadel, *The Hippocampus as a Cognitive Map* (Clarendon, Oxford, 1978).
- H. Eichenbaum, P. Dudchenko, E. Wood, M. Shapiro, H. Tanila, *Neuron* **23**, 209 (1999).
- B. L. McNaughton, R. G. M. Morris, *Trends Neurosci.* **10**, 408 (1987).
- J. O'Keefe, J. Dostrovsky, *Brain Res.* **34**, 171 (1971).
- R. U. Muller, J. L. Kubie, J. B. Ranck, *J. Neurosci.* **7**, 1935 (1987).
- B. L. McNaughton, C. A. Barnes, J. O'Keefe, *Exp. Brain Res.* **52**, 41 (1983).
- J. J. Knierim, H. S. Kudrimoti, B. L. McNaughton, *J. Neurosci.* **15**, 1648 (1995).
- J. O'Keefe, D. H. Conway, *Exp. Brain Res.* **31**, 573 (1978).
- K. M. Gothard, W. E. Skaggs, B. L. McNaughton, *J. Neurosci.* **16**, 8027 (1996).
- M. L. Shapiro, H. Tanila, H. Eichenbaum, *Hippocampus* **7**, 624 (1997).
- E. R. Wood, P. A. Dudchenko, H. Eichenbaum, *Nature* **397**, 613 (1999).
- E. J. Markus *et al.*, *J. Neurosci.* **15**, 7079 (1995).
- M. A. Moita, S. Rosis, Y. Zhou, J. E. LeDoux, H. T. Blair, *J. Neurosci.* **24**, 7015 (2004).
- E. R. Wood, P. A. Dudchenko, R. J. Robitsek, H. Eichenbaum, *Neuron* **27**, 623 (2000).
- J. Ferbinteanu, M. L. Shapiro, *Neuron* **40**, 1227 (2003).
- M. R. Bower, D. R. Euston, B. L. McNaughton, *J. Neurosci.* **25**, 1313 (2005).
- S. A. Hollup, S. Molden, J. G. Donnett, M.-B. Moser, E. I. Moser, *J. Neurosci.* **21**, 1635 (2001).
- E. Bostock, R. U. Muller, J. L. Kubie, *Hippocampus* **1**, 193 (1991).
- C. Kentros *et al.*, *Science* **280**, 2121 (1998).
- A. Cressant, R. U. Muller, B. Poucet, *Exp. Brain Res.* **143**, 470 (2002).
- D. Marr, *J. Physiol.* **202**, 437 (1969).
- S. Leutgeb, J. K. Leutgeb, A. Treves, M.-B. Moser, E. I. Moser, *Science* **305**, 1295 (2004); published online 22 July 2004 (10.1126/science.1100265).
- Materials and methods are available as supporting material on Science Online.
- The mean number of pretraining days in the test environment was 17 (square-circle), 14 (two rooms), and 4 (black-white).
- The rate threshold was 0.27 Hz. Similar results were obtained with rate thresholds of 0.10 Hz and 0.50 Hz (tables S1 and S2) (23).
- K. M. Gothard, W. E. Skaggs, K. M. Moore, B. L. McNaughton, *J. Neurosci.* **16**, 823 (1996).
- W. E. Skaggs, B. L. McNaughton, *J. Neurosci.* **18**, 8455 (1998).
- H. Tanila, *Hippocampus* **9**, 235 (1999).
- If the external spatial input is strong enough, it is theoretically possible for large changes to occur in the firing rates of some cells, whereas intrinsic attractor dynamics of the network maintain the relative relations between the place fields of the ensemble (35).
- S. A. Hollup, S. Molden, J. G. Donnett, M.-B. Moser, E. I. Moser, *Eur. J. Neurosci.* **13**, 1197 (2001).
- In these studies, which all focused on CA1, much of the residual activity in the less active condition appeared inside the cell's place field in the more active condition [e.g., figure 8 in (30), figures 3 to 5 in (14), figures 2 to 6 in (15), figure 6 in (16), figures 6B and 9 in (12), and figure 4 in (13)], as expected if the remapping was primarily rate-based. In (30), 70% of the cells exhibited peak activity in the same quadrant in the two directions.
- T. J. Wills, C. Lever, F. Cacucci, N. Burgess, J. O'Keefe, *Science* **308**, 873 (2005).
- H. Markram, M. Tsodyks, *Nature* **382**, 807 (1996).
- E. Tulving, *Annu. Rev. Psychol.* **53**, 1 (2002).
- A. Samsonovich, B. L. McNaughton, *J. Neurosci.* **17**, 5900 (1997).
- We thank R. G. M. Morris and M. P. Witter for discussion and A. M. Amundsgård, I. M. F. Hammer, K. Haugen, K. Jenssen, R. Skjerpeng, E. Sjulstad, B. H. Solem, and H. Waade for technical assistance. The work was supported by a Centre of Excellence grant from the Norwegian Research Council.

### Supporting Online Material

www.sciencemag.org/cgi/content/full/309/5734/619/DC1

Materials and Methods  
Figs. S1 to S5  
Tables S1 and S2

25 April 2005; accepted 10 June 2005  
10.1126/science.1114037

## Complete Replication of Hepatitis C Virus in Cell Culture

Brett D. Lindenbach,<sup>1</sup> Matthew J. Evans,<sup>1</sup> Andrew J. Syder,<sup>1</sup> Benno Wölk,<sup>1</sup> Timothy L. Tellinghuisen,<sup>1</sup> Christopher C. Liu,<sup>2</sup> Toshiaki Maruyama,<sup>3\*</sup> Richard O. Hynes,<sup>2</sup> Dennis R. Burton,<sup>3</sup> Jane A. McKeating,<sup>1†</sup> Charles M. Rice<sup>1‡</sup>

Many aspects of the hepatitis C virus (HCV) life cycle have not been reproduced in cell culture, which has slowed research progress on this important human pathogen. Here, we describe a full-length HCV genome that replicates and produces virus particles that are infectious in cell culture (HCVcc). Replication of HCVcc was robust, producing nearly  $10^5$  infectious units per milliliter within 48 hours. Virus particles were filterable and neutralized with a monoclonal antibody against the viral glycoprotein E2. Viral entry was dependent on cellular expression of a putative HCV receptor, CD81. HCVcc replication was inhibited by interferon- $\alpha$  and by several HCV-specific antiviral compounds, suggesting that this *in vitro* system will aid in the search for improved antivirals.

HCV is a major cause of chronic liver disease, with over 170 million persistently infected individuals worldwide (1). HCV-associated

liver disease frequently progresses to cirrhosis, which can lead to liver failure and hepatocellular carcinoma. Current drug therapies are often poorly tolerated and effective in only a fraction of patients; there is no vaccine for HCV. A major obstacle to understanding the virus life cycle and to developing improved therapeutics is the inability to efficiently grow HCV in cell culture.

HCV is an enveloped, positive-sense RNA virus of the family *Flaviviridae*. Naturally occurring variants of HCV are classified into six major genotypes. The 9.6-kb genome encodes one large polyprotein that is processed by viral and cellular proteinases to produce the virion structural proteins (core and glycoproteins E1 and E2) as well as nonstructural (NS)

proteins (p7 through NS5B) (Fig. 1A). Subgenomic RNA replicons have been adapted for efficient RNA replication in the human hepatoma line Huh-7 and other cultured cells (2–5). However, full-length genomes containing cell culture-adaptive mutations do not produce infectious virus particles in culture and are severely attenuated *in vivo* (6–8). This led us to hypothesize that mutations that enhance RNA replication may have deleterious effects on virion production. To test this idea, we used a genotype 2a subgenomic replicon, SGR-JFH1, that efficiently replicates in cell culture without adaptive mutations (4). Full-length chimeric genomes were constructed with the use of the core-NS2 gene regions from the infectious J6 (genotype 2a) and H77 (genotype 1a) virus strains (Fig. 1A). Both full-length chimeras and the subgenomic RNA were competent for RNA replication, as seen by the accumulation of NS5A protein and viral RNA 48 hours after RNA transfection into the Huh-7.5 cell line (Fig. 1B). As expected, mutation of the NS5B RNA polymerase active site [GlyAspAsp to GlyAsnAsp (GND)] destroyed the ability of FL-J6/JFH to replicate (Fig. 1B). Within transfected cells, both full-length genomes expressed core, E2, and NS5A (Fig. 1C). As expected, SGR-JFH1 expressed NS5A but not core or E2. While  $\approx 30\%$  of cells were productively transfected with FL-J6/JFH, FL-H77/JFH, or SGR-JFH1 RNA (Fig. 1B),  $>95\%$  of FL-J6/JFH-transfected cells were positive for NS5A by 96 hours (fig. S1). This suggested that FL-J6/JFH spread within the transfected cell cultures.

To test whether infectivity could be transferred to naïve cells, we clarified conditioned

<sup>1</sup>Center for the Study of Hepatitis C, The Rockefeller University, 1230 York Avenue, New York, NY 10021, USA. <sup>2</sup>Howard Hughes Medical Institute, Center for Cancer Research, Massachusetts Institute of Technology, Cambridge, MA 02139, USA. <sup>3</sup>Departments of Immunology and Molecular Biology, The Scripps Research Institute, La Jolla, CA 92037, USA.

\*Present address: Alexion Antibody Technologies, San Diego, CA 92121, USA.

†Present address: Division of Immunity and Infection, Institute of Biomedical Research, University of Birmingham Medical School, Birmingham B15 2TT, UK.

‡To whom correspondence should be addressed. E-mail: ricec@rockefeller.edu